

# Enhancing MOTION2NX for Efficient, Scalable and Secure Image Inference using Convolutional Neural Networks

Haritha K<sup>1</sup>, Ramya Burra<sup>2</sup>, Srishti Mittal<sup>1</sup>, Sarthak Sharma<sup>1</sup>, Abhilash Venkatesh<sup>1</sup>, and Anshoo Tandon<sup>1</sup>

<sup>1</sup> IUDX, Bengaluru, India

{gattu.haritha, srishti.mittal413, sarthaksharma070, abhilashnitk3, anshoo.tandon}@gmail.com

<sup>2</sup> CBR, IISc, Bengaluru  
ramya.burra@gmail.com

**Abstract.** This work contributes towards the development of an efficient and scalable open-source Secure Multi-Party Computation (SMPC) protocol on machines with moderate computational resources. We use the ABY2.0 SMPC protocol implemented on the C++ based MOTION2NX framework for secure convolutional neural network (CNN) inference application with semi-honest security. Our list of contributions are as follows. Firstly, we enhance MOTION2NX by providing a tensorized version of several primitive functions including the Hadamard product, indicator function and argmax function. Our design of secure indicator function based on a novel approach that uses secure Relu function available in the baseline MOTION2NX implementation. The secure indicator function is used, in turn, as a building block for a novel implementation of secure argmax. Secondly, we also develop a novel splitting of the computations at each CNN layer into multiple configurable chunks thereby resulting in significant reduction in RAM usage. Thirdly, we adapt an existing Helper node algorithm, working in tandem with the ABY2.0 protocol, for efficient convolution computation. This algorithm not only reduces execution time but also reduces the RAM usage required to execute CNN models, but comes at a cost of an additional compute server. Moreover, the ideas presented in this paper can also be applied to secure neural network training.

**Keywords:** SMPC, ABY2.0, MOTION2NX.

## 1 Introduction

In today's interconnected and data-driven world, the ability to perform computations while preserving privacy and security is paramount. Privacy is considered a fundamental human right as it balances the need for transparency and accountability with the protection of individual rights [1]. As technology advances and the digital age evolves, preserving privacy remains a pressing concern

that requires ongoing attention and protection. Secure Multi Party Computation (SMPC) serves as a fundamental tool to address these concerns and facilitates secure data sharing and decision-making across various domains. When implementing SMPC for real-life data, it is essential to consider factors such as the nature of the data, the privacy requirements, the computational resources available, and the specific tasks to be performed. In this paper, our objective is to tackle the challenge of implementing the SMPC protocol in real world scenarios and at scale on machines with modest computational resources, all while striving to minimize the execution time. Our main goal is to optimize the code, making it more efficient and accessible to a broader audience, ultimately empowering SMPC. We offer neural network inference solutions with semi-honest security [11] executed on virtual machines with less than 1 GB RAM. Previous baseline implementation required 8.03 GB RAM on virtual machines for executing the same neural network model [6]. In practical real-world setting, this reduction in RAM usage results in significant cost reduction (in dollar terms) [3].

To accomplish this, we modified the C++ based MOTION2NX framework [5] and included additional functionality to provide a *resource-optimized* implementation for secure inferencing tasks. We begin by examining MOTION2NX’s limitations, such as memory issues and the lack of interoperability between tensor and non-tensor operations. The proposed enhancements include leveraging efficient tensor operations, overcoming the absence of an argmax function using novel approaches, optimizing memory usage, and reducing execution time with the introduction of a third-party Helper node. These improvements aim to enhance the framework’s capabilities and efficiency while maintaining data privacy and integrity (refer to Section 3 for details).

In our optimized implementation, it is important to highlight that the memory usage of a standard  $N$ -layer neural network is determined by its largest layer, i.e., the layer with most parameters. *This feature makes our implementation highly scalable as the memory footprint does not grow with the number of layers of the neural network.* Moreover, we present an approach to further decrease the memory footprint by splitting the computations for the largest layer without compromising on privacy or accuracy.

We use the data provider framework of SMPC. We consider two compute servers (for executing the ABY2.0 SMPC protocol [10]) and two data providers (that actually possess input data and neural network model, respectively). Data providers provide shares to compute servers for computation in this framework (see Section 2.3 for details). We assume that the readers are familiar with ABY2.0 protocol [10].

## 1.1 Related Work

Over the past several years, there has been an increased focus on practical application of SMPC to real-world problems. Here, we elucidate two real-life applications of SMPC.

*Secure Auction* In Denmark, farmers sell sugar beets to Danisco. The Market Clearing Prices, which represent the price per unit of the commodity that balances total supply and demand in the auction, play a pivotal role in the allocation of contracts among farmers, ensuring a fair and efficient distribution of production rights. To preserve bid privacy in this process, a three-party SMPC system involving representatives from Danisco, and two other organizations was employed [4].

*Secure Gender Wage Gap Study* Here, a specialized software facilitates data analysis of collaborative compensation for organizations, like the Boston Women’s Workforce Council (BWWC) study in Greater Boston [9]. This application seamlessly integrates SMPC techniques to ensure collective computation of aggregate compensation data while preserving individual privacy. This approach empowers organizations to collaborate effectively while upholding data privacy.

We remark that the above two described SMPC applications are not memory or computationally intensive. On the other hand, in this paper, we present the modifications and functional additions to the MOTION2NX framework for practical implementation of secure neural network inference task that is *both* memory intensive and computationally intensive. These modifications and updates are a step towards secure disease prediction (see [2] for secure medical image analysis) where one party provides secret shares of medical images while the other party provides secret shares of a pre-trained neural network model.

## 1.2 Our Contributions

The following is the list of our contribution, specifically to MOTION2NX setup.

- We enhance MOTION2NX by providing a tensorized version of several primitive functions including the Hadamard product, indicator function and argmax function. Our design of secure indicator function based on a novel approach that uses secure Relu function available in the baseline MOTION2NX implementation. The secure indicator function is used, in turn, as a building block for a novel implementation of secure argmax.
- We develop a novel splitting of the computations at each CNN layer into multiple configurable chunks thereby resulting in significant reduction in RAM usage.
- We adapt an existing Helper node algorithm, working in tandem with the ABY2.0 protocol, for efficient convolution computation. This algorithm not only reduces execution time but also reduces the RAM usage required to execute CNN models, but comes at a cost of an additional compute server.
- Further, our implementation of the secure indicator function can be used to design secure piece-wise linear approximation of a given function. In particular, we design a 5–piece approximation of sigmoid function that can be used during neural network training.

The source code of our optimized implementations along with docker images is available at <https://github.com/datakaveri/iudx-MOTION2NX>.

## 2 Preliminaries

In this section, we provide preliminary details of our secure neural network inferring implementation.

### 2.1 Framework for Implementation

We consider MOTION2NX, a C++ framework for generic mixed-protocol secure two-party computation in our paper. The following are the features of baseline MOTION2NX.

- Assumes data providers are a part of compute servers
- No intermediate values are reconstructed
- Assumes either of the compute servers as output owners
- Output is reconstructed in clear and shared with the output owner

*Tensor and non-Tensor variants:* MOTION2NX offers non-optimized secure functions that compile the descriptions of low-level circuits, which are referred to as non-tensor operations. MOTION2NX also provides optimized building blocks that directly implement common high-level operations, which are referred to as tensor operations. The tensor operations are computationally efficient than the primitive operations. MOTION2NX uses a specialized executor to evaluate the tensor operations sequentially while parallelizing the operations with multi-threading and SIMD operations

We discuss the details of our proposed enhancements and optimizations in Section 3.

### 2.2 $N$ -layer Convolutional Neural Network

Our optimizations in MOTION2NX enable efficient execution of deep Convolutional neural networks. For illustrative purposes, we present the details for 4-layer and 6-layer convolutional neural networks (CNN) on MNIST and CIFAR-10 datasets, respectively. A similar procedure can be adapted for any other dataset on their pre-trained models with multiple CNN layers.

In MNIST inference task, the input to the neural network is a real-valued vector. The output is an integer  $i \in \{0 \dots 9\}$ . For illustrative purposes, we consider 4 - layer model with two convolution layers and two fully connected layers MNIST dataset inferring task with parameters as described in Table 1. Algorithm 1 describes a simple two convolution layer and two neural network layer inference implementation with ReLU activation in secure mode. This algorithm takes ABY2.0 shares of input data (image), network weights, and biases as inputs and produces ABY2.0 shares of the predicted label as output. The image shares, weight shares and bias shares at server- $i$ ,  $i \in \{0, 1\}$  are represented as  $x^i$ ,  $w_j^i$  and  $b_j^i$ ,  $j \in \{1, 2, 3, 4\}$  respectively. Further,  $w_1^i$  and  $w_2^i$  represent the kernel parameters for CNN layers while  $w_3^i$  and  $w_4^i$  represent matrix parameters for fully connected neural network layers.

Table 1: Neural Network Configuration used for Inferencing MNIST Data

| Layer | No. of Kernels | Padding      | Strides | No. of parameters              | Biases         |
|-------|----------------|--------------|---------|--------------------------------|----------------|
| CNN1  | 5              | (1, 0, 1, 0) | (2,2)   | $5 \times 1 \times 5 \times 5$ | $5 \times 1$   |
| CNN2  | 3              | (1, 0,1,0)   | (1,1)   | $3 \times 5 \times 4 \times 4$ | $3 \times 1$   |
| NN1   | 100 neurons    | -            | -       | $108 \times 100$               | $100 \times 1$ |
| NN2   | 10 neurons     | -            | -       | $100 \times 10$                | $10 \times 1$  |

We recall that ABY2.0 shares consist of a pair comprising a public share and a private share [10]. For instance, the ABY2.0 shares of an input variable  $y$  associated with server  $i$  are represented as a pair consisting of  $\Delta_y$  and  $[\delta_y]_i$ . Note that  $\Delta$  and  $\delta$  represent public share and private share respectively.

---

**Algorithm 1** CNN inferencing task with ReLU activation function at compute server- $i$ ,  $i \in \{0, 1\}$

---

**Require:** Input image shares  $x^i$ , weight shares  $w_1^i, w_2^i, w_3^i, w_4^i$ , bias shares  $b_1^i, b_2^i, b_3^i, b_4^i$ .

All the above shares are vectors in the form of ABY2.0 shares

**Ensure:** Shares of predicted class label  $\hat{y}^i$

- 1: Compute first layer:
  - 2:  $z_1^i = \text{SecureCNN}(w_1^i, x^i, b_1^i)$
  - 3:  $h_1^i = \text{SecureReLU}(z_1^i)$
  - 4: Compute Second layer:
  - 5:  $z_2^i = \text{SecureCNN}(w_2^i, h_1^i, b_2^i)$
  - 6:  $h_2^i = \text{SecureReLU}(z_2^i)$
  - 7: Compute Third layer:
  - 8:  $z_3^i = \text{SecureAdd}(\text{SecureMul}(w_3^i, h_2^i), b_3^i)$
  - 9:  $h_3^i = \text{SecureReLU}(z_3^i)$
  - 10: Compute Forth layer:
  - 11:  $z_4^i = \text{SecureAdd}(\text{SecureMul}(w_4^i, h_3^i), b_4^i)$
  - 12:  $h_4^i = \text{SecureReLU}(z_4^i)$
  - 13: Compute predicted class label:
  - 14:  $\hat{y}^i = \text{SecureArgmax}(h_4^i)$
  - 15: **Return**  $\hat{y}^i$
- 

We remark that the steps outlined in Algorithm 1 can be readily extended to secure execution of general deep CNN inferencing tasks (with any number of layers). Most of the secure functions listed in Algorithm 1 were provided by MOTION2NX framework. We used ABY2.0 arithmetic protocol for convolution, multiplication and addition. We used Yao protocol to perform the ReLU function, as Yao performs better for comparison operations. Algorithm 1, unfortunately, couldn't be executed completely in MOTION2NX using its baseline built-in functions as SecureArgmax was not available. We enhance the MOTION2NX framework by implementing a tensorized version of the SecureArgmax function as explained in Algorithm 5 in Section 4. This marks a departure from

the previous approach [6], where the authors relied on a non-tensor version of SecureArgmax to achieve a similar functionality.

### 2.3 Data Provider Model

In this model the data providers (Image provider and Model provider) create shares of their private data and communicate them with the compute servers for further computation. Compute servers perform the inference task and send the output shares to the Image provider. Compute servers are unaware of the clear output result. For secure inference task, we consider that the neural network model is pretrained and is proprietary to a model provider. Similarly, the image for the inference task is private to image data provider [6].

## 3 Optimizations on Inference Time and Memory Usage

In this section we explain how we optimize memory usage and inference time.

### 3.1 Optimizing Memory Requirement

In the context of secure inference tasks using the MNIST dataset, we observed a substantial RAM requirement of approximately 0.2 GB (per server instance) for a 4-layer neural network. In practical terms, this RAM demand poses a significant obstacle to performing inference tasks on a resource constrained machine. This issue is further aggravated when we work with a neural network with relatively large number of layers and real time datasets, e.g. x-ray images. To address this challenge, our primary objective was to reduce the memory requirement, thereby facilitating the use of more complex neural networks.

In the specific context of a 4-layer neural network inference model (Table 1), the major memory requirement arises from the matrix multiplication in layer-3 and convolution operation in layer-1. To mitigate the memory usage by matrix multiplication operation the authors in [6] proposed intra-layer optimization where the matrix multiplication task is implemented in smaller segments (or "splits"), resulting in a proportional decrease in the average RAM requirement. In this work, we propose executing the convolution operation kernel by kernel, which we refer to as a vertical split (CNNV Split) in the further discussion of the paper. It is evident from Table 5 that the average RAM requirement decreases as we execute convolution kernel by kernel at each layer. We discuss in detail about optimizing memory in Section 5.

### 3.2 Optimizing Execution Time using Helper Node Algorithm

Our next objective was to optimize the execution time. For secure convolution and matrix multiplication, the execution time is significantly impacted by the use of oblivious transfers (OTs) which occur behind the scenes. To address this issue, we use a semi-honest third-party Helper node that eliminates the need for

OTs during convolution. For detail discussion on Helper-node Algorithm please see [6].

The Helper-node algorithm, reduces the inference time from 20.7 seconds (for the baseline implementation with no intra-layer optimization on a 4-layer neural network) to 15.2 sec. Additionally, the RAM requirement reduced from 0.219 GB to 0.042 GB (see Table 5). Note that, while the Helper node functionality reduces both execution time and RAM usage, it requires the addition of a third server (Helper node), increasing the server count from two to three.

## 4 Enhancements to MOTION2NX Framework

In this section, we discuss about the functions integrated into the MOTION2NX framework. Our observation revealed the absence of certain functions necessary for executing neural network training and inference tasks, e.g., Hadamard product (element-wise multiplication of matrices), indicator function, and sigmoid function. Additionally, due to the unavailability of  $\exp(\cdot)$ , implementing the sigmoid function proved challenging. Consequently, we opted for a 5-piece approximation of the sigmoid function [8]. The implementation of this approximation necessitated the incorporation of auxiliary functions, specifically, Hadamard product and indicator function.

### 4.1 Hadamard Product :

Let  $\langle a \rangle$  and  $\langle b \rangle$  represent the ABY2.0 shares of matrices  $a$  and  $b$  respectively, and let  $a \odot b$  denote the Hadamard product of  $a$  and  $b$ . We implemented Hadamard product on these matrices as explained in Algorithm 2. Further, we extended this implementation to accommodate scenarios where matrix  $a$  is in clear form while matrix  $b$  is in ABY2.0 shares. Note that, **OT** block represents oblivious transfer that occurs during multiplication.

---

#### Algorithm 2 Protocol SecureHamm( $\langle a \rangle, \langle b \rangle$ )

---

- 1: **Setup Phase:**
  - 2: Each party  $P_i, i \in \{0, 1\}$  compute the following
  - 3:  $[\Delta_y]_i = [\delta_a]_i \odot [\delta_b]_i$
  - 4:  $[\Delta_y]_i = [\Delta_y]_i + \mathbf{OT}([\delta_a]_i \odot [\delta_b]_{1-i}) + \mathbf{OT}([\delta_a]_{1-i} \odot [\delta_b]_i)$
  - 5: **Online Phase:**
  - 6: Each party  $P_i, i \in \{0, 1\}$  compute the following
  - 7:  $[\Delta_y]_i = [\Delta_y]_i - [\Delta_a] \odot [\delta_b]_i - [\Delta_b] \odot [\delta_a]_i$
  - 8:  $[\Delta_y]_i = [\Delta_y]_i + i * ([\Delta_a] \odot [\Delta_b])$
  - 9: perform truncation operation on  $[\Delta_y]_i$
  - 10:  $[\Delta_y]_i = [\Delta_y]_i + [\delta_y]_i$ , where  $[\delta_y]_i \in_R \mathbb{Z}_2^{64}$
  - 11:  $P_i$  sends  $[\Delta_y]_i$  to  $P_{1-i}$
  - 12: Both  $P_0$  and  $P_1$  calculate  $\Delta_y = [\Delta_y]_0 + [\Delta_y]_1$
-

*Remark 1.* Implementing the **OT** block for the Hadamard product is not straightforward. To achieve this, we first studied how **OT** is implemented for matrix multiplication in the existing MOTION2NX framework. Then, we made the necessary modifications to adapt it for the Hadamard product.

## 4.2 Indicator :

Let  $I()$  denote indicator function in clear, we implemented its secured version by leveraging the SecureRelu(.) function provided in the MOTION2NX framework, as detailed below. The indicator function in clear  $I()$  is given below.

$$I(x) = \begin{cases} 0 & \text{if } x < 0, \\ 1 & \text{otherwise.} \end{cases} \quad (1)$$

We use the Relu function as a building block to implement the indicator function (1). This is achieved by first constructing an approximate indicator function as follows,

$$\text{ApproxInd}(x) = \text{Relu}(1 - K \text{Relu}(-x)) \quad (2)$$

where  $K > 2^{13}$ . We plot  $\text{ApproxInd}(x)$  for  $K = 2^{14}$  in Fig.1 for  $-1 \leq x \leq 1$ . Note that,  $\text{ApproxInd}(x)$  can also be written as

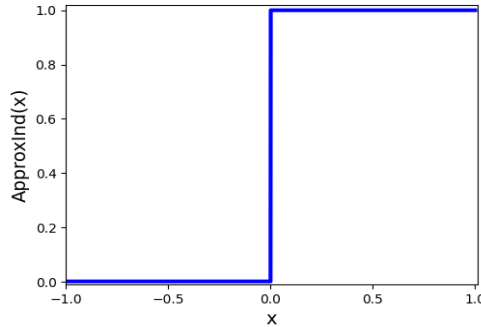


Fig. 1:  $\text{ApproxInd}(x)$  for  $K = 2^{14}$

$$\text{ApproxInd}(x) = \begin{cases} 0, & \text{if } x < -\frac{1}{K}, \\ 1 + Kx, & \text{if } -\frac{1}{K} \leq x \leq 0, \\ 1 & \text{if } x > 0. \end{cases} \quad (3)$$

Further, MOTION2NX uses the ring  $\mathbb{Z}^{64}$  for arithmetic operations. It supports 64 bit fixed point arithmetic including  $f$  bits to represent the fraction part of variable  $x$ . In our implementation we chose  $f = 13$ .



When  $x$  is a fixed point number (with  $f = 13$  bits for the fractional part) and  $K > 2^f = 2^{13}$  then comparing (1) and (3), we observe that  $I(x) = \text{ApproxInd}(x)$ . This means that our  $\text{ApproxInd}(x)$  does not result in any approximation error.

Using the above ideas we implement the secure version of the Indicator function as follows.

$$\text{SecureInd}(x) = \text{SecureRelu}(1 - K \text{SecureRelu}(-x)), \quad (4)$$

where  $K > 2^f$ ,  $f$  is number of fractional bits.

We remark that  $\text{SecureInd}()$  can intern be use dto implement secure piece-wise linear approximation of sigmoid function as explained in the following.

### 4.3 Piece-wise linear approximation of sigmoid :

We implemented the 5-piece linear approximation of sigmoid function described in [8]. Towards this first we present the details of 5-piece approximation from [8] and subsequently we present the algorithm we employed to implement the same in secure manner.

$$\text{SigmApprox}(x) = \begin{cases} 10^{-4}, & \text{if } x < -5, \\ 0.02776x + 0.145, & \text{if } -5 \leq x < -2.5, \\ 0.17x + 0.5, & \text{if } -2.5 \leq x < 2.5, \\ 0.02776x + 0.85498, & \text{if } 2.5 \leq x < 5, \\ 1 - 10^{-4}, & 5 \leq x. \end{cases} \quad (5)$$

The sigmoid function is approximated with a 5-piece model, utilizing five linear equations as depicted in (5). Let  $m_j, c_j, j \in \{1, \dots, 5\}$ , where  $m_1 = 0, m_2 = 0.02776, m_3 = 0.17, m_4 = 0.02776, m_5 = 0$  and  $c_1 = 10^{-4}, c_2 = 0.145, c_3 = 0.5, c_4 = 0.85498, c_5 = 1 - 10^{-4}$ , denote slopes and intercepts respectively the linear equations described in (5). Further, let  $I_j, j \in \{1, \dots, 5\}$  be the intervals corresponding to the linear equations in (5). Also, we denote the upper limits of the intervals using  $u_j, j \in \{1, \dots, 5\}$  where  $u_1 = -5, u_2 = -2.5, u_3 = 2.5, u_4 = 5, u_5 = \infty$ . This notation aids in the implementation of the secure version of 5-piece sigmoid approximation as described in Algorithm 4.

We briefly explain Algorithm 4. Let  $x^i, i \in \{0, 1\}$  be the Boolean ABY2.0 shares of the input vector. Note that,  $t_j, d_j, z_j, k_j, p_j, j \in \{1 \dots 5\}$  defined in Algorithm 4 have the length same as input vector. Now we compute the interval to which the input belongs to using  $\text{SecureInd}()$  and  $\text{SecureHamm}()$  functions in steps 2-10. For example, if a value belongs to the  $I_5$ , then corresponding secure values  $z_5^i, i \in \{0, 1\}$  give one in clear, all other  $z_j^i, j \in \{1, 2, 3, 4\}$  secure values give zero in clear. Subsequently, we multiply with corresponding slopes of the linear equation that is active in the interval and add the intercept (steps 12-17). For better understanding we present the same in clear and we map the steps between the clear implementation and secure implementation.

---

**Algorithm 3** SigmApprox :Clear Implementation of Computing 5-piece sigmoid approximation

---

**Require:** Array of input valyes  $x$  in clear

**Ensure:** 5-piece-wise approximation of sigmoid function for the input  $\hat{y}$

- 1: Compute the interval to which  $x$  belongs to :
  - 2: **for**  $j = 1, j \leq 4$  **do**
  - 3:      $t_j = \text{Indicator}(x - u_j)$
  - 4: **end for**
  - 5: Let  $z_j, j \in \{1, \dots, 5\}$  be arrays that hold the information about which interval each element in  $x$  belongs to:
  - 6:      $z_1 = 1 - t_1$
  - 7: **for**  $j = 2, j \leq 4$  **do**
  - 8:      $d_j = 1 - t_j$
  - 9:      $z_j = d_j \odot t_{j-1}$
  - 10: **end for**
  - 11:      $z_5 = t_4$
  - 12: Using the slopes, intercepts and interval information we compute the 5-piece approximation of sigmoid
  - 13:  $k_1 = m_1 * x + c_1$
  - 14:  $p_1 = k_1 \odot z_1$
  - 15: **for**  $j = 2, j \leq 5$  **do**
  - 16:      $k_j = m_j * x + c_j$
  - 17:      $p_j = p_{j-1} + z_j \odot k_j$
  - 18: **end for**
  - 19:  $\hat{y} = p_5$
  - 20: **Return**  $\hat{y}$
-

---

**Algorithm 4** SecureSigmApprox : Computing 5-piece sigmoid approximation values for an array of inputs  $x^i$  at compute server- $i$ ,  $i \in \{0, 1\}$

---

**Require:** Boolean ABY2.0 shares of input  $x^i$

**Ensure:** Shares of 5-piece sigmoid approximated values  $\hat{y}^i$

- 1: Compute the interval to which each element in  $x_i$  belongs to :
  - 2: **for**  $j = 1, j \leq 4$  **do**
  - 3:      $t_j^i = \text{SecureInd}(\text{SecureConstAdd}(-u_j, x^i))$
  - 4: **end for**
  - 5: Let  $z_j^i, j \in \{1, \dots, 5\}$  be arrays that hold the information about which interval each element in  $x^i$  belongs to:
  - 6:      $z_1^i = \text{SecureConstAdd}(1, \text{SecureNegate}(t_1^i))$
  - 7: **for**  $j = 2, j \leq 4$  **do**
  - 8:      $d_j^i = \text{SecureConstAdd}(1, \text{SecureNegate}(t_j^i))$
  - 9:      $z_j^i = \text{SecureHamm}(d_j^i, t_{j-1}^i)$
  - 10: **end for**
  - 11:      $z_5^i = t_4^i$
  - 12: Using the slopes, intercepts (in clear) and interval information (in shares) we compute the 5-piece approximation of sigmoid
  - 13:  $k_1^i = \text{SecureConstAdd}(c_1, \text{SecureConstMult}(m_1, x^i))$
  - 14:  $p_1^i = \text{SecureHamm}(z_1^i, k_1^i)$
  - 15: **for**  $j = 2, j \leq 5$  **do**
  - 16:      $k_j^i = \text{SecureConstAdd}(c_j, \text{SecureConstMult}(m_j, x^i))$
  - 17:      $p_j^i = \text{SecureAdd}(p_{j-1}^i, \text{SecureHamm}(z_j^i, k_j^i))$
  - 18: **end for**
  - 19:  $\hat{y}^i = p_5^i$
  - 20: **Return**  $\hat{y}^i$
-

#### 4.4 Argmax :

We implement tensor version of argmax as explained in Algorithm 5 and compare the execution times of scalar and tensor versions of argmax for inputs with different lengths (see Table 2). The input to SecureArgmax is a boolean ABY2.0 shares tensor and output is the first index at which the maximum element is present.

In Step 1, we determine the maximum value in the input array of length  $n$  using the SecureMaxpool function. It is important to note that the input and output of this function are Boolean shares, which should be converted into arithmetic shares to proceed. In Step 2, we create an array of length  $n$  where each element equal to the maximum value computed in Step 1. Subsequently, in Step 3, we subtract this array from the input array, and in Step 4, we pass the result to an indicator function. At this stage, we have an array with zeros and ones, where the positions of ones indicate the presence of the maximum value in the input array. Moving on to Step 6, we perform a Hadamard multiplication of the array obtained from Step 4 with  $0, 1, \dots, n - 1$ . Note that, the non-zero elements present in  $z_4^i$  are the indices at which the maximum element is present. However, we only need one index, we choose the maximum no-zero index available by executing SecureMaxpool on it, as outlined in Step 7. Additionally, we compare the execution time of scalar and tensor versions of argmax in Table 2.

---

**Algorithm 5** SecureArgmax : Computation of the index of the maximum element in the input array at compute server- $i, i \in 0, 1$

---

**Require:** Boolean ABY2.0 shares of input vector  $x^i$  and its length  $n$

**Ensure:** Shares of the index of a maximal element  $\hat{y}^i$

- 1: Compute the shares of the maximum element  $z_1^i$  as  $z_1^i = \text{SecureMaxPool}(x^i)$
  - 2: Let  $t$  be all ones vector of size  $n$ . Create an array  $z_2^i$  of size  $n$  as  $z_2^i = \text{SecureConstMatrixMult}(z_1^i, t)$
  - 3: Subtract the maximum value from the input array:  $z_3^i = \text{SecureAdd}(x^i, \text{SecureNegate}(z_2^i))$
  - 4: Compute the array with zeros and ones, where one represents the presence of maximum element at that position:  $z_4^i = \text{SecureIndicator}(z_3^i)$
  - 5: Let  $k = \{0, 1, \dots, n - 1\}$ . Compute the argmax shares by executing the following two steps:
  - 6:  $z_5^i = \text{SecureConstHamm}(k, z_4^i)$
  - 7:  $\hat{y}^i = \text{SecureMaxPool}(z_5^i)$
  - 8: **Return**  $\hat{y}^i$
- 

In Table 2, we provide the execution times for the scalar and vectorized versions of Argmax. The vector version was introduced in Algorithm 5, while the scalar version was detailed in our earlier work [6]. To facilitate a comparison between the scalar and tensor versions, we input vectors of varying lengths and measure the execution times. Evidently, it is apparent that the tensor version of Argmax exhibits lower execution times in comparison to the scalar version.

Table 2: Comparison of Argmax Execution Time in Scaler and Tensor Versions

| Vector Length | Execution Time (sec) |                |
|---------------|----------------------|----------------|
|               | Scalar Version       | Tensor Version |
| 100           | 11.23                | 4.46           |
| 200           | 22.95                | 5.025          |
| 300           | 35.6                 | 8              |
| 400           | 73.7                 | 11.2           |
| 500           | 154                  | 25.25          |
| 600           | 201.5                | 30.8           |
| 700           | 255                  | 32.05          |
| 800           | 365                  | 32.8           |

## 5 Numerical Results:

In this section, we illustrate the RAM usage and execution time taken by Algorithm 1 on MNIST and CIFAR-10 datasets. Towards this, first we explain the setup for the execution and subsequently the challenges we encountered in image inferencing and the techniques we employed to overcome.

In practice, the compute servers are typically hosted on the cloud (on different LANs). To determine the execution time, we deployed compute server 0 on Microsoft Azure cloud and compute server 1 (and the Helper node) on AWS cloud (see Table 3). The image provider and weights/model provider run on separate local machines.

Table 3: Cloud Configuration

|                  |   |
|------------------|---|
| Server 0         | Azure: b1s 1vcpu, 1 GB RAM, 30 GB SSD     |
| Server 1         | AWS: t2.micro 1vcpu, 1 GB RAM, 30 GB SSD  |
| Helper node      | AWS: t2.nano 1vcpu, 0.5 GB RAM, 30 GB SSD |
| Image provider   | Personal laptop                           |
| Weights provider | Personal laptop                           |

We executed Algorithm 1 on MNIST and CIFAR-10 datasets. Observe that, the network configuration we used in MNIST dataset inferencing (see Table 1) is a small network model compared with the actual network models that are used in real world image inferencing applications. Towards this, we considered image inferencing on CIFAR-10 dataset with the network configuration shown in Table 4 that is closer to real world image inferencing tasks. Further, we observed that the image inferencing tasks using Algorithm 1 on MNIST dataset consumed 0.219 GB RAM (see first row in Table 5) and we could not execute the same on CIFAR-10 dataset with the specified RAM resources on cloud (see first row in Table 6). To meet the RAM requirements, we proposed memory optimization techniques, which are discussed below. Towards this, we consider inferencing

MNIST task and explain how convolution layer parameters affect the RAM usage and using the proposed technique how RAM usage can be decreased.

Table 4: Neural Network Configuration used for Inferring CIFAR-10 Data

| Layer | No. of Kernels | padding     | strides    | weights                          | Biases         |
|-------|----------------|-------------|------------|----------------------------------|----------------|
| CNN1  | 32             | 1,1         | 1, 1, 1, 1 | $32 \times 3 \times 5 \times 5$  | $32 \times 1$  |
| CNN2  | 32             | 1, 1, 1, 1  | 1,1        | $32 \times 32 \times 5 \times 5$ | $32 \times 1$  |
| CNN3  | 64             | 2, 2, 2, 2, | 2, 2       | $64 \times 32 \times 5 \times 5$ | $64 \times 1$  |
| CNN4  | 64             | 0, 0, 0, 0  | 1,1        | $64 \times 64 \times 3 \times 3$ | $64 \times 1$  |
| NN1   | 100 neurons    | -           | -          | $108 \times 512$                 | $512 \times 1$ |
| NN2   | 10 neurons     | -           | -          | $512 \times 10$                  | $10 \times 1$  |

We have detailed the model used in inferencing task on MNIST data in Algorithm 1. It is important to note that the RAM required for computing  $z_j^i, h_j^i, j \in \{1, \dots, 4\}$  in a single process increases with the size of the input data, number of kernels, and the number of weights at the network layers. Furthermore, executing the inferencing task may be impractical in restricted resource environments. To address this, we computed  $z_j^i, h_j^i, j \in \{1, \dots, 4\}$  in 8 processes sequentially and saved the output shares from each process to a file. This process ensures that each executing process operates on the output shares written by the previous process, preventing any data leakage. We observed both the RAM usage and execution time for each process. Additionally, we noted that computing  $h_j^i, j \in \{1, \dots, 4\}$  (SecureRelu) consumes less RAM compared to the computation of  $z_j^i, j \in \{1, \dots, 4\}$  (SecureMul, SecureCNN). The first entry in Table 1 denotes the maximum RAM usage among all 8 processes along with the corresponding process’s execution time. Now, we elaborate on the number of multiplications to be performed to compute output of each layer. Towards this, first we introduce the formulae to compute dimensions and the number of multiplications to be performed to compute each element in the output of the convolution layer.

The input and output of the convolution layer are three-dimensional matrices. For a given set of input dimensions and convolution layer parameters, the output dimensions are computed using (6). Here,  $i_{ch}$ ,  $i_{row}$ , and  $i_{col}$  represent the number of channels, rows, and columns in the input, while  $str$ ,  $pad$ ,  $n_{ker}$ ,  $k_{row}$ , and  $k_{col}$  represent convolution parameters strides, padding, number of kernels, number of rows, and number of columns in the kernel, respectively. Additionally,  $o_{ch}$ ,  $o_{row}$ , and  $o_{col}$  signify the number of channels, rows, and columns of the convolution layer’s output. The number of channels at the output of a convolution layer is equal to the number of kernels used at the same the convolution layer, i.e.,  $o_{ch} = n_{ker}$ , and the number of rows and columns at convolution layer’s output are calculated using (6) [7].

$$\begin{aligned}
o_{row} &= \left\lfloor \frac{i_{row} + pad[0] + pad[1] - k_{row}}{str[0]} \right\rfloor + 1 \\
o_{col} &= \left\lfloor \frac{i_{col} + pad[2] + pad[3] - k_{col}}{str[1]} \right\rfloor + 1
\end{aligned} \tag{6}$$

We supply MNIST data with dimensions  $i_{ch} = 1$ ,  $i_{row} = 28$ , and  $i_{col} = 28$  as input to CNN1. Using (6), we compute the output dimensions of CNN1 and CNN2, for the parameters outlined in Table 5. The resulting output dimensions for CNN1 are  $o_{ch} = 5$ ,  $o_{row} = 13$ , and  $o_{col} = 13$ . For each element in the output of CNN1, the number of multiplications to be performed is  $i_{ch} \times k_{row} \times k_{col}$ , which is equal to  $1 \times 5 \times 5 = 25$ . The total number of elements in the output of CNN1  $o_{ch} \times o_{rows} \times o_{col}$ , which is equal to  $5 \times 13 \times 13 = 845$ . So the total number of multiplications required to compute the output of CNN1 is  $25 \times 845 = 21,125$ . Following the same procedure, we compute the output dimensions of CNN2 as  $3 \times 6 \times 6$ , with a total of 8,640 multiplications (see the first row in Table 5). Now, the output of CNN2 is flattened to dimensions  $108 \times 1$  and acts as input to NN1, which has weight dimensions of  $100 \times 108$ . Computing  $\text{SecureMul}(w_3^i, h_3^i)$  at NN1 involves  $100 \times 108 = 10,800$  multiplications. Similarly, the number of multiplications at NN2 ( $\text{SecureMul}(w_4^i, h_4^i)$ ) is computed as  $100 \times 10 = 1,000$ . Now we know the number of multiplications to be performed at each layer we study the effect of number of multiplications on RAM usage.

In MOTION2NX framework, each multiplication operation entails OT transfers that utilize RAM. As illustrated in Table 5, the RAM usage increases with an increase in the number of multiplications, posing a challenge to scaling. To address this scaling issue in the convolution layer, we adopt a kernel-by-kernel split approach, conducting computations for each kernel individually in a sequence instead of computing for all kernels at once. After convolution operation with each kernel, we save the output shares to a file. Upon completing the convolution operation for all kernels, we concatenate the output shares obtained kernel-wise sequentially, creating a final output share file. For example, consider the first convolution layer that has 5 kernels. We execute the convolution in 5 splits. In this scenario, 5 processes are executed sequentially, and output shares from each process are saved and concatenated in the end.

We have two convolution layers CNN1 and CNN2 with number of kernels equal to 5 and 3 respectively. We execute inferring task using different split configurations for the model described in Table 1 and tabulate RAM usage and execution times in Table 5. Note that, these values correspond to the maximum of RAM and the maximum execution time among all the processes that executed during the inferring task. Further, the first column gives us the split configuration we used at the convolution layers and second column gives the number splits at the neural network layers. For example, CNNV split = (5, 1) refers to we executed convolution operation at CNN1 and CNN2 in 5 and 1 processes respectively. This means, we executed convolution operation at CNN1, kernel by kernel sequentially

i.e., we stored the output shares of convolution with kernel  $k, k \in \{1, 2, 3, 4\}$  before executing the convolution operation with kernel  $k + 1$  and we executed the whole convolution operation in one go at CNN2. Further, NN split = (20, 2) means we executed matrix multiplication at NN1 and NN2 in 20 and 1 processes respectively.

*Remark 2.* In any layer, whether it be a convolution or a fully connected neural network layer, having a single split means that all computations related to that layer are computed in a single process.

To examine the impact of splits on convolutional layers, we explored various split configurations and calculated the corresponding RAM usage and execution times, as shown in Table 5. A noteworthy observation was that, for a given number of multiplications, matrix multiplication consumes more RAM than convolution operations. To clarify this, consider the first and second entries for the CNNV Split and NNSplit configurations: (1, 1), (1, 1) and (1, 1), (20, 2), respectively. In the first entry, the maximum number of multiplications occurs in CNN1 (=21, 125) among the convolution layers and in NN1 (=10, 800) among the neural network layers, with RAM usage of 0.219 GB. Let’s assume that CNN1 predominantly contributes to the overall RAM usage. In the second entry, the execution is split at NN1 and NN2 (NNSplit = (20, 10)) with no split at CNN1 and CNN2. If CNN1 were responsible for the maximum RAM usage, then the RAM usage in the second entry would not have decreased. However, we observe a reduction in RAM usage to 0.092 GB, indicating that NN1, despite having fewer multiplications (10, 800) compared to CNN1 (21, 125), is the primary driver of RAM consumption.

In third, fourth and fifth entries we use NNSplit = (20, 2), but changed splits at convolution layers and indicated the split (CNNV and the number of multiplications that drives the RAM usage in bold). We clearly observe that as the number of multiplications reduced the RAM usage also reduced. Furthermore, in the fourth and fifth entries, we observe that the maximum number of multiplications are 21, 125 and 4, 225, with corresponding RAM usage of 0.109 GB and 0.035 GB, respectively. Interestingly, although the number of multiplications decreases by a factor of five, the RAM usage does not scale down proportionally. This is because, regardless of the number of multiplications performed during convolution, a fixed portion of RAM is allocated.

Note that, images in MNIST dataset are monochrome, with only one input channel, and we utilized a minimal number of kernels (five and three) at CNN1 and CNN2 layers. In contrast, typical input images have three channels (RGB: Red, Green, Blue), and convolution layers often employ a larger number of kernels (e.g., 64, 128). To demonstrate the computational load when considering an RGB image as an input and a more realistic number of kernels at convolution layers, we examine the CIFAR-10 dataset and the neural network model described in Table 4.

In our attempt to execute the inference task, we allocated 1 GB of memory but encountered failure due to insufficient memory when no splits were applied



Table 5: Ram Usage and Execution Time for Different Split Configurations for MNIST Data Inferring Task

| split configuration |         | No. of multiplications |              |               |      | LAN      |            | WAN      |            |
|---------------------|---------|------------------------|--------------|---------------|------|----------|------------|----------|------------|
| CNNV split          | NNSplit | CNN1                   | CNN2         | NN1           | NN2  | RAM (GB) | time (sec) | RAM (GB) | time (sec) |
| (1, 1)              | (1,1)   | 21,125                 | 8,640        | <b>10,800</b> | 1000 | 0.219    | 19.1       | 0.219    | 20.7       |
| (1, 1)              | (20,2)  | <b>21,125</b>          | 8,640        | 540           | 500  | 0.092    | 31.1       | 0.089    | 42.4       |
| (5, 1)              | (20,2)  | 4,225                  | <b>8,640</b> | 540           | 500  | 0.057    | 26.3       | 0.058    | 50.2       |
| (1, 3)              | (20,2)  | <b>21,125</b>          | 2,880        | 540           | 500  | 0.109    | 20.3       | 0.109    | 46.5       |
| (5, 3)              | (20,2)  | <b>4,225</b>           | 2,880        | 540           | 500  | 0.035    | 43.1       | 0.036    | 54.3       |
| Helper node         |         | 21,125                 | 8,640        | 10,800        | 1000 | 0.042    | 14.1       | 0.042    | 15.2       |

at the convolution layers. Recognizing this limitation, in the subsequent configuration, denoted as the second entry, we implemented a split configuration of CNNV Split = (32, 32, 64, 64), NN Split = (256, 5), resulting in a RAM usage of 0.548 GB. Note that, we computed convolution output for each kernel in a different process and appended the outputs to get the final convolution output and the appended them to get the final output. With this strategy, the minimum RAM required to execute is 0.548 GB. To reduce it further, we introduced a strategy of splitting the input to the convolution layer into smaller chunks and perform convolution. We explain this in detail in Section 5.

In the third configuration, we reduced the number of splits at CNN2 from 32 to 16 while maintaining other parameters constant. However, this adjustment led to a notable increase in RAM usage to 1.077GB, nearly doubling from the second configuration. Additionally, we observed that the number of multiplications performed at CNN2 surpassed those in other convolution layers, acting as a bottleneck for RAM usage.

Table 6: Ram Usage and Execution Time for Different Split Configurations for CIFAR-10 Dataset Inferring Task

| split configuration |          | No. of multiplications |                       |                       |                       |                      |                      | WAN      |            |
|---------------------|----------|------------------------|-----------------------|-----------------------|-----------------------|----------------------|----------------------|----------|------------|
| CNNV Split          | NN Split | CNN1<br>$\times 10^3$  | CNN2<br>$\times 10^3$ | CNN3<br>$\times 10^3$ | CNN4<br>$\times 10^3$ | NN1<br>$\times 10^3$ | NN2<br>$\times 10^3$ | RAM (GB) | Time (sec) |
| (1, 1, 1, 1)        | (1,1)    | 878                    | 5,760                 | 3,276                 | 1,327                 | 1179                 | 5                    | -        | -          |
| (32, 32, 64, 64)    | (256, 5) | 27.6                   | 180                   | 51.2                  | 20.7                  |                      |                      | 0.548    | 1097       |
| (32, 16, 64, 64)    | (256, 5) | 27.6                   | 360                   | 3,276                 | 1,327                 |                      |                      | 1.077    | 1118       |
| <b>Helper node</b>  | -        | 878                    | 5,760                 | 3,276                 | 1,327                 | 1179                 | 5                    | 0.725    | 82         |

**Horizontal Split :** In this section we explain the technique we used to reduce the RAM usage further. From Table 6, we observe that executing convolution on each kernel individually requires 0.548 GB of RAM for the inference task on

the CIFAR-10 dataset. It’s important to note that while the CIFAR-10 dataset has an input image size of  $3 \times 32 \times 32$ , typical image sizes for practical inference tasks are significantly larger. Consequently, the minimum RAM requirement also increases. To address this, we not only perform convolution kernel by kernel but also divide the input data at the convolution layer into smaller chunks. We then perform the convolution sequentially on these smaller input data chunks and append the outputs obtained from each chunk to form the final output. Further, as we split the total number of rows present in input data into smaller chunks and thus we call this horizontal splitting. We explain this in detail in Algorithm6.

The inputs to Algorithm 6 are the number of rows in one input channel of the convolution layer in, padding values, stride values and number of splits (partitions) on the convolution input. The output of Algorithm6 is start and end row indices of the input data. Further, for each start index and end index, we read corresponding data from the input on which convolution has to be performed and supply as input to SecureConv(.) function. We write the output of SecureConv(.) to an output file for further computation.

## 6 Conclusion and Future Work

We modified and enhanced the MOTION2NX framework to bridge the gap between scalability, memory efficiency and privacy. In particular, we optimized the memory usage, reduced the execution time using a third-party Helper node, and enhanced the efficiency while still preserving data privacy. These optimizations enable CIFAR-10 dataset inference in just 32 seconds with only 0.7 GB of RAM for a four layer CNN. In contrast, the previous baseline implementation required more than 1000 seconds of execution time and 8 GB of RAM. Our next objective is to use Helper node for implementing activation functions and solving linear optimization on ABY 2.0 framework.

## References

1. 494/2012, C.N.W.C.: Fundamental right to privacy (2021), <https://www.scobserver.in/cases/puttaswamy-v-union-of-india-fundamental-right-to-privacy-case-background/>, <https://www.scobserver.in/cases/puttaswamy-v-union-of-india-fundamental-right-to-privacy-case-background/>, Accessed: 2023-09-25
2. Alvarez-Valle, J., Bhatu, P., Chandran, N., Gupta, D., Nori, A., Rastogi, A., Rathee, M., Sharma, R., Ugare, S.: Secure medical image analysis with cryptflow (2020), arXiv,2012.05064
3. Amazon: VPS, web hosting pricing (2023), <https://aws.amazon.com/lightsail/pricing/>
4. Bogetoft, P., Christensen, D.L., Damgård, I., Geisler, M., Jakobsen, T.P., Krøigaard, M., Nielsen, J.D., Nielsen, J.B., Nielsen, K., Pagter, J.I., Schwartzbach, M.I., Toft, T.: Secure multiparty computation goes live. In: Financial Cryptography (2009), <https://api.semanticscholar.org/CorpusID:3608554>

---

**Algorithm 6** Horizontal Split : Computation of the start and end row indices for the input data

---

**Input :** Padding values  $[p_0, p_1, p_2, p_3]$ , stride values  $[s_0, s_1]$ , number of rows in each input channel  $d_r$ , number of rows in each kernels  $k_r$ , number of kernels  $n_k$ , number of horizontal splits  $n_h$

**Output :** Start and end row indices of input data to the convolution layer that accounts for padded rows

```

1: Compute the effective number of rows after padding
2:    $D_r = d_r + p_0 + p_1$ 
3: Compute the number of rows per channel at the output of the convolution :
4:    $o_r = \lfloor \frac{D_r - k_r}{s_0} \rfloor + 1$ 
5: Compute the number of output rows for each input horizontal split given at the
   convolution layer, except the last one:
6:    $h_r = \lfloor \frac{o_r}{n_h} \rfloor$ 
7: Compute the start and end row indices of the input data at the convolution layer
   that accounts for padded rows:
8:    $S_r = 0$                                      ▷ row start indices
9:    $E_r = 0$                                        ▷ row end indices
10:   $t = 0$ 
11: for  $i \in \{1 \dots n_h\}$  do
12:   if  $i == n_h$  then
13:      $h_r = \lfloor \frac{o_r}{n_h} \rfloor + o_r \bmod n_h$ 
14:   end if
15:   if  $i == 1$  then
16:      $S_r[i] = 1$ 
17:   else
18:      $S_r[i] = t - (K_r - 1) + s_0$ 
19:   end if
20:    $E_r[i] = S_r[i] + (k_r - 1) + (h_r - 1) * s_0$ 
21:    $t = E_r[i]$ 
22: end for

```

---

5. Braun, L., Cammarota, R., Schneider, T.: A generic hybrid 2PC framework with application to private inference of unmodified neural networks (extended abstract). In: NeurIPS 2021 Workshop Privacy in Machine Learning (2021), <https://openreview.net/forum?id=CXFh9utHuw2>
6. Burra, R., Tandon, A., Mittal, S.: Empowering SMPC: bridging the gap between scalability, memory efficiency and privacy in neural network inference. In: 16th International Conference on COMMunication Systems & NETWORKS, COMSNETS 2024, Bengaluru, India, January 3-7, 2024. pp. 1–6. IEEE (2024). <https://doi.org/10.1109/COMSNETS59351.2024.10427509>, <https://doi.org/10.1109/COMSNETS59351.2024.10427509>
7. Dumoulin, V., Visin, F.: A guide to convolution arithmetic for deep learning (2018)
8. Hong, C., Huang, Z., Lu, W.j., Qu, H., Ma, L., Dahl, M., Mancuso, J.: Privacy-preserving collaborative machine learning on genomic data using tensorflow. In: Proceedings of the ACM Turing Celebration Conference - China. p. 39–44. ACM TURC '20, Association for Computing Machinery, New York, NY, USA (2020). <https://doi.org/10.1145/3393527.3393535>, <https://doi.org/10.1145/3393527.3393535>
9. Lapets, A., Dunton, E., Holzinger, K., Jansen, F., Bestavros, A.: Web-based multi-party computation with application to anonymous aggregate compensation analytics (2015), <https://open.bu.edu/handle/2144/21773>
10. Patra, A., Schneider, T., Suresh, A., Yalame, H.: ABY2.0: Improved Mixed-Protocol secure Two-Party computation. In: 30th USENIX Security Symposium (USENIX Security 21). pp. 2165–2182. USENIX Association (Aug 2021), <https://www.usenix.org/conference/usenixsecurity21/presentation/patra>
11. Veugen, T., Blom, F., de Hoogh, S.J.A., Erkin, Z.: Secure comparison protocols in the semi-honest model. IEEE Journal of Selected Topics in Signal Processing **9**(7), 1217–1228 (2015). <https://doi.org/10.1109/JSTSP.2015.2429117>